

Development of reduced activation austenitic stainless steel containing high density of nanosized precipitates for fusion energy application

Date: Oct. 22nd, 2021

Time: 11:30 ~ 11:50

Hyun Joon Eom, Ji Ho Shin, Byeong Seo Kong,
Chae Won Jeong, Changheui Jang* (KAIST)

Nuclear & High Temperature Materials Laboratory
Department of Nuclear & Quantum Engineering, KAIST

Contents

I. Introduction

II. Alloy design

- Part I: Chemical composition

- Part II: Thermo-mechanical processing (TMP)

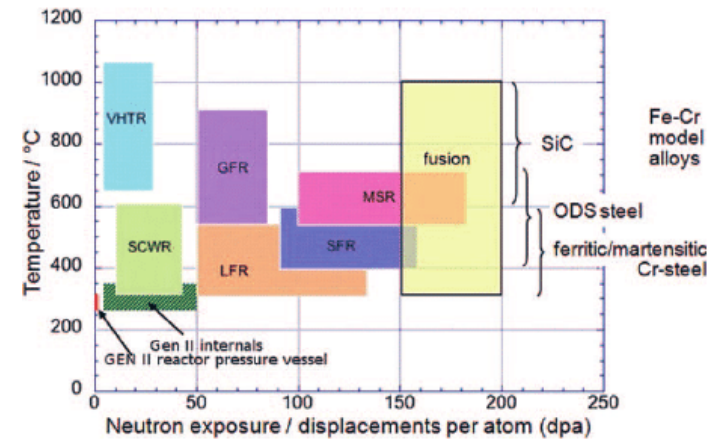
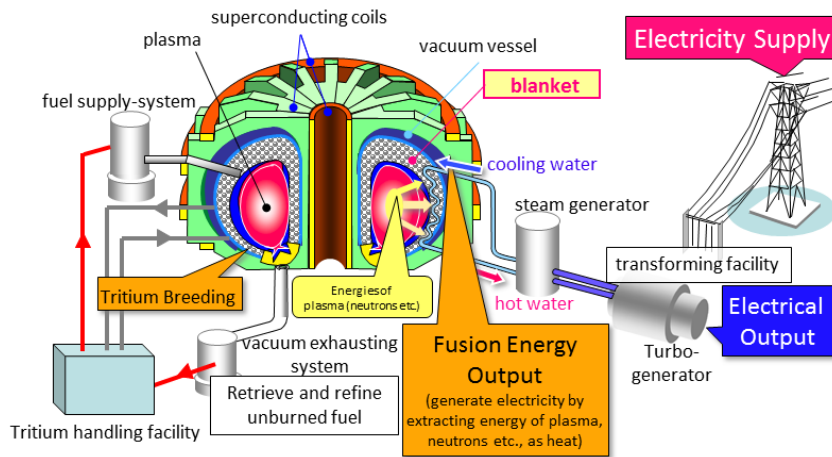
III. Irradiation experiment

IV. Results

V. Summary

❑ Schematic of Fusion Reactor

- High temperature & high neutron irradiation environment



▲ Operating condition for various nuclear reactors [1]

❑ Operating condition for blanket

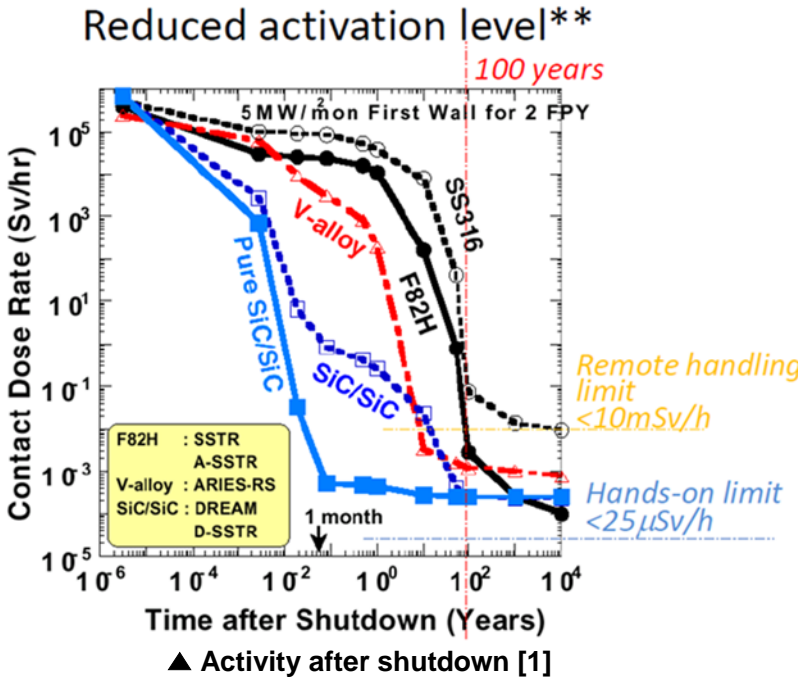
- Temperature: $\sim 300 - \sim 700$ °C
- Neutron irradiation: $\sim 150 - \sim 200$ dpa

❑ Requirement for blanket structural materials

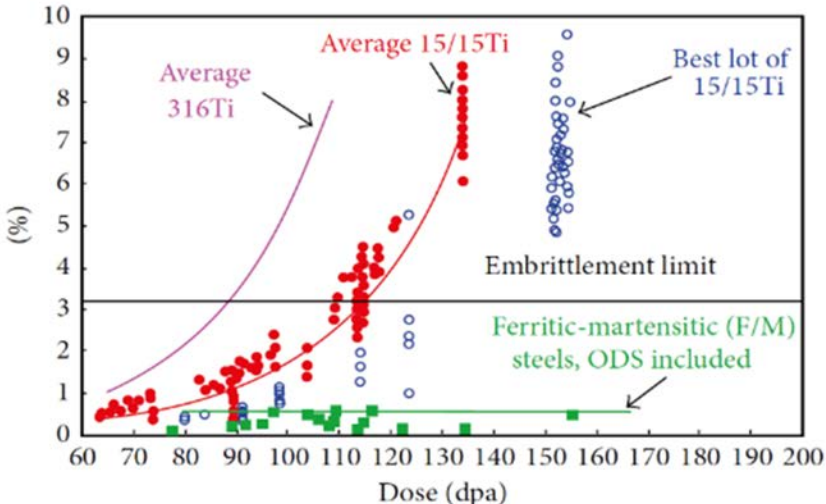
- **Low activation material**
- Good high-temperature mechanical property
- Good irradiation resistance (e.g. radiation embrittlement & void swelling resistance)
- Compatibility with chemicals (coolant, breeding material)

Candidate material for blanket in nuclear fusion reactor

	Reduced activation	Irradiation resistance		Corrosion resistance	High temperature property	Magnetic property
		Embrittlement	Swelling			
FMS&FM-ODS	Good	Poor	Good	Poor	Good	Ferromagnetic
Austenitic SS (316)	Poor	Good	Poor	Good	Good	Paramagnetic



▲ Comparison between FMS&FM-ODS and austenitic SS (316)



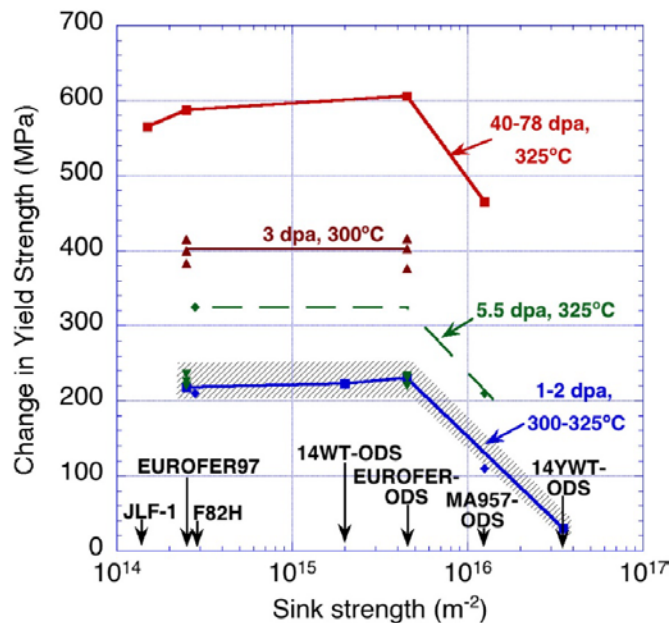
▲ Void swelling resistance for various alloys [2]



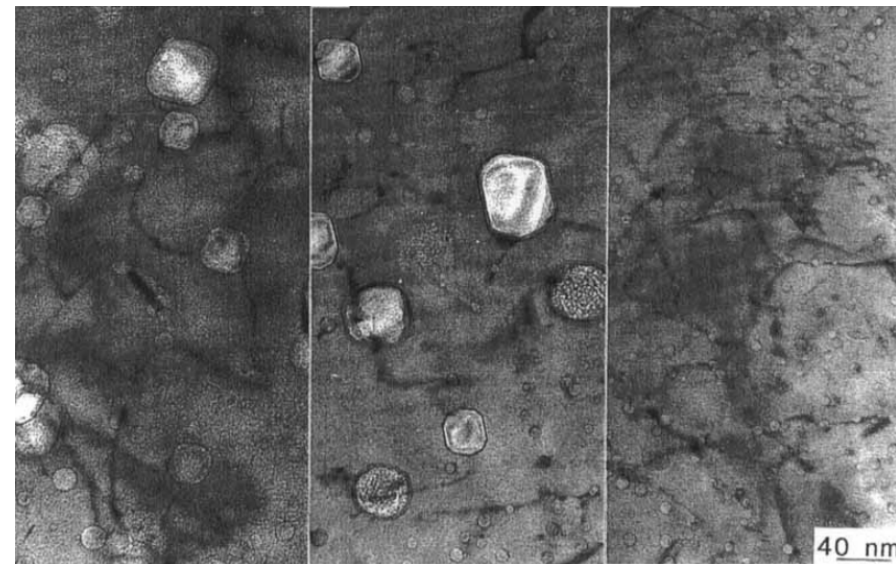
Development of **A**dvanced radiation **R**esistant austenitic stainless **S**teel for **F**usion reactor in-core materials (**ARES-F**)

□ Enhancing irradiation resistance of **ARES-F**

- Trap He to avoid void swelling
- Recombination of radiation-induced defects
- High **sink strength** : Ability to absorb the radiation damage
 - Precipitate sink strength $\rightarrow S_{ppt} = 4\pi r \rho_{ppt} [m^{-2}]$
 - Dislocation sink strength $\rightarrow S_{dis} \propto \rho_{dis} [m^{-2}]$
- Good thermo-mechanical properties at severe environment (Fusion reactor)



▲ Effect of sink strength on radiation damage [1]



Increasing number density of precipitates

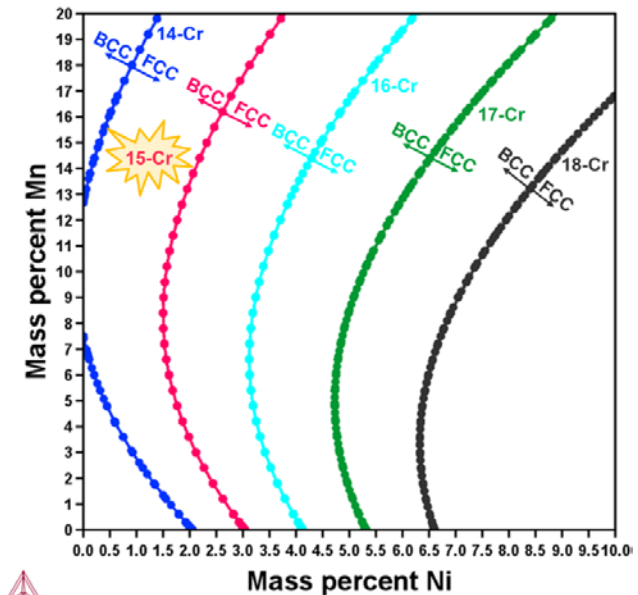
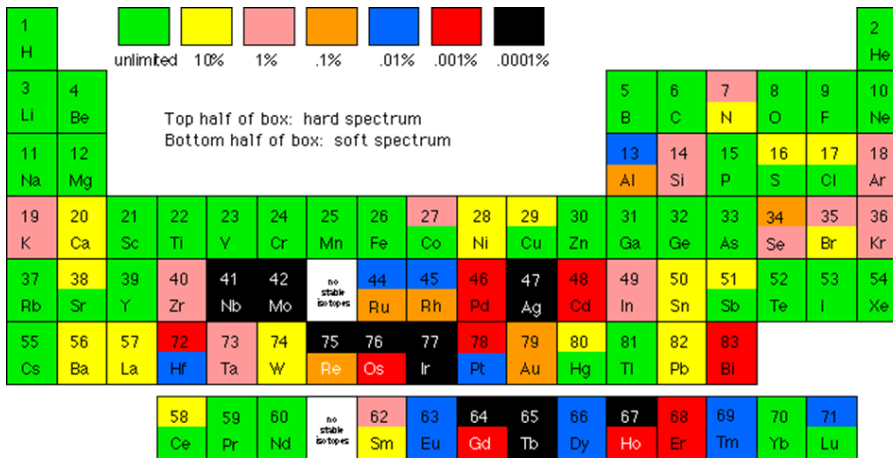
▲ Void swelling resistance by precipitation [2]

Alloy design – Chemical composition

[1] S. J. Zinkle, Fusion Sci. and Tech. 64 (2013) 65

Chemical composition for **ARES-F**

- Limitation on content for reduced activation
 - Replacement of **Ni** with **Mn**
 - Consideration of **long-term waste disposal**
- Alloy design based on thermodynamic simulation modeling (Thermo-Calc.)
 - Database : TCFE-9 (steels/Fe-alloys v9.0) & MOBFE3 (steels/Fe-alloys mobility v3.0)
 - Fe-Cr-Ni-Mn system
 - **Cr > 15 wt.%** for enough **corrosion resistance**



▲ Reduced activation elements based on the long term waste disposal criteria [1]



▲ Ni-Mn balance for stable austenitic matrix based on Thermo-Calc.

Alloy design – Chemical composition

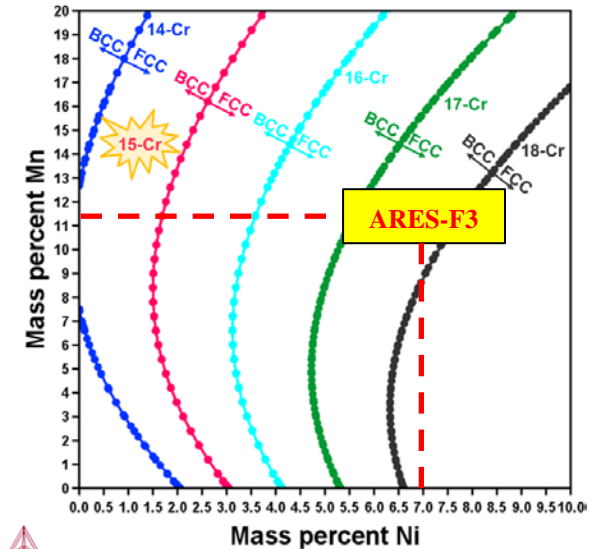
Chemical composition for ARES-F

[1] R.E. Schram et al., Metallurgical Transactions A. (1975) 1345
 [2] A.F. Padilha et al., ISIJ International. (2002) 325

- Stable austenitic matrix with Fe-Cr-Ni-Mn system
 - Stacking fault energy [$mJ \cdot m^{-2}$] – [1]
 - $\rightarrow \gamma_{SF} = -53 + 6.2(wt. \%Ni) + 0.7(wt. \%Cr) + 3.2(wt. \%Mn)$
 - Martensite formation temperature [$^{\circ}C$] – [2]
 - $\rightarrow M_s = 1302 - 42(wt. \%Cr) - 61(wt. \%Ni) - 33(wt. \%Mn) - 28(wt. \%Si) - 1667(wt. \%C + wt. \%N)$

Optimization of key element chemical composition

- Reference alloy : 304 SS & 316 SS
- Stacking fault energy: $> 30 mJ \cdot m^{-2}$
- Martensite formation temperature: $< -200^{\circ}C$



▲ Ni-Mn balance for stable austenitic matrix based on Thermo-Calc.

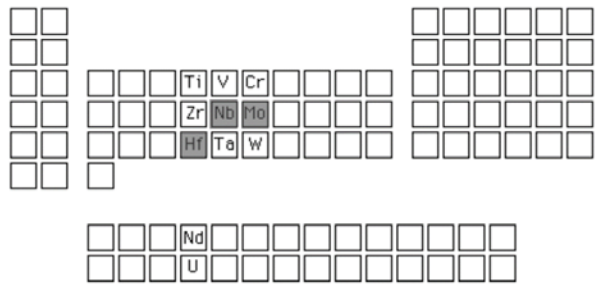
	Fe	Cr	Ni	Mn	Stacking fault energy [$mJ \cdot m^{-2}$]	Martensite formation temperature [$^{\circ}C$]
304 SS	Bal.	18.29	8.06	1.05	13.1	-133.4
316 SS	Bal.	17.09	10.28	0.58	44.5	-211.0
ARES-F3	Bal.	15	7	11.3	37.1	-200.2

▲ Chemical composition and corresponding stacking fault energy and martensite formation temperature of 304 SS, 316 SS and ARES-F3

Alloy design – Chemical composition

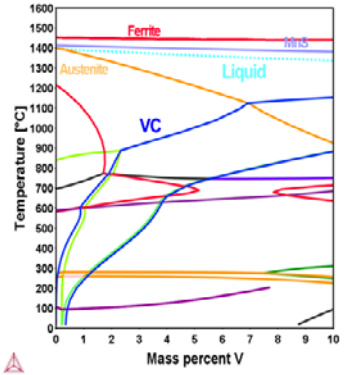
[1] H.K.D.H Bhadeshia, (2000) Proc. of 5th Inter. Charles Par. Tur. Conf., UK

□ Precipitation for ARES-F3

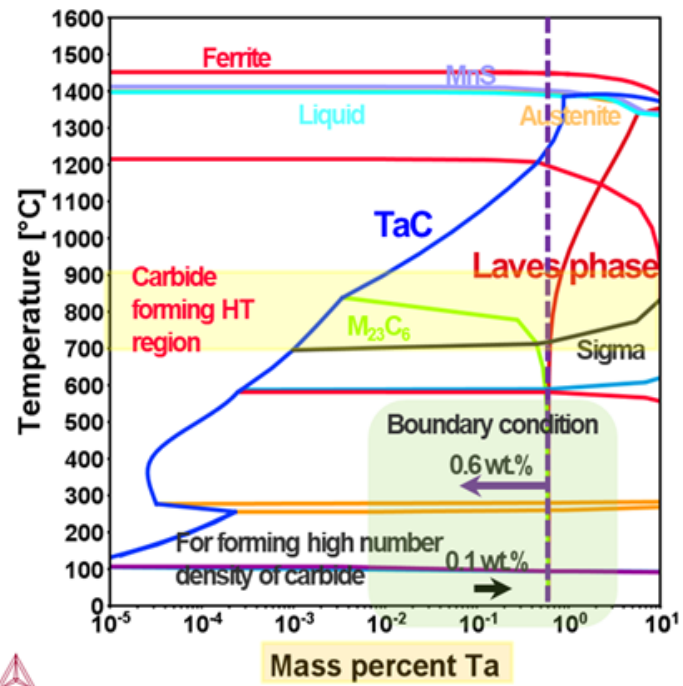


▲ Strong carbide forming element [1]

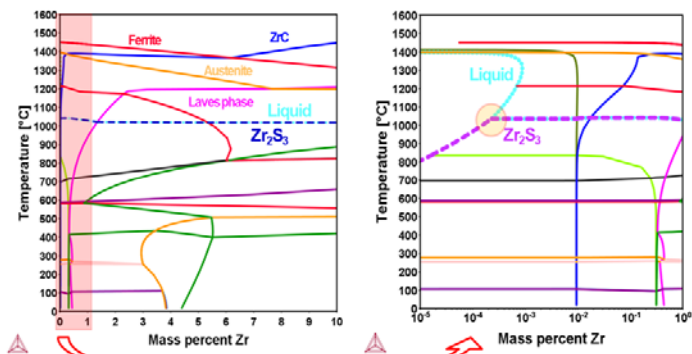
- Standard for minor alloying element for precipitation
 - Easy to control by heat treatment (**carbide** vs. **nitride**)
 - Low diffusivity → Large number of fine precipitates
 - Matrix stability → Thermo-Calc. simulation
- Vanadium carbide
 - **Unstable matrix**
- Zirconium carbide
 - **Unstable matrix**
- Tantalum carbide
 - **Stable matrix**



▲ Phase diagram for VC precipitate



▲ Phase diagram for TaC precipitate



▲ Phase diagram for ZrC precipitate

Alloy design – Chemical composition

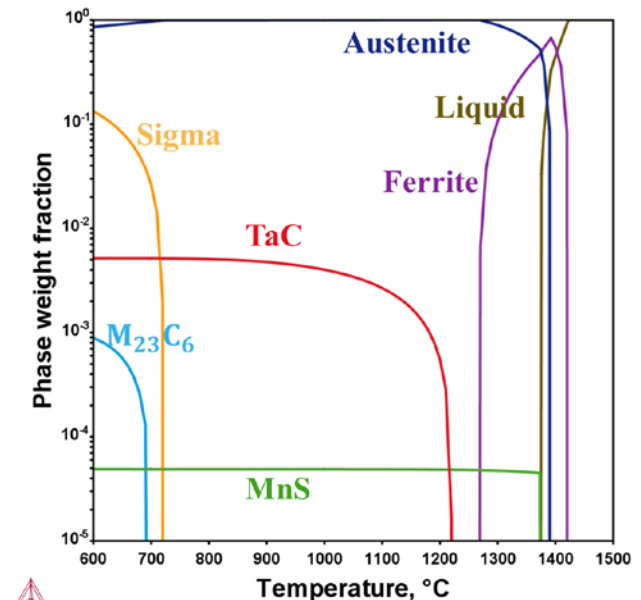
☐ ARES-F3

- Austenitic matrix + TaC precipitates
- Low activation material with high sink strength
- Target chemical composition : Fe – 15Cr – 7Ni – 11.3Mn – 0.45Ta – 0.04C (wt.%)

	Fe	Cr	Ni	Mn	Ta	C	Si	P	S
ARES-F3	Bal.	15.13	7.17	11.16	0.48	0.039	0.22	0.001	0.002

▲ Inductively Coupled Plasma Atomic Emission Spectroscopy (ICP-AES) for ingot of ARES-F3 (wt.%)

- Thermodynamic simulation modeling (Thermo-Calc.)
 - TCFE-9 (steels/Fe-alloys v9.0)
 - MOBFE3 (steels/Fe-alloys mobility v3.0)
 - Minimization of Si content to prevent TaC coarsening
 - P & S content → impurities



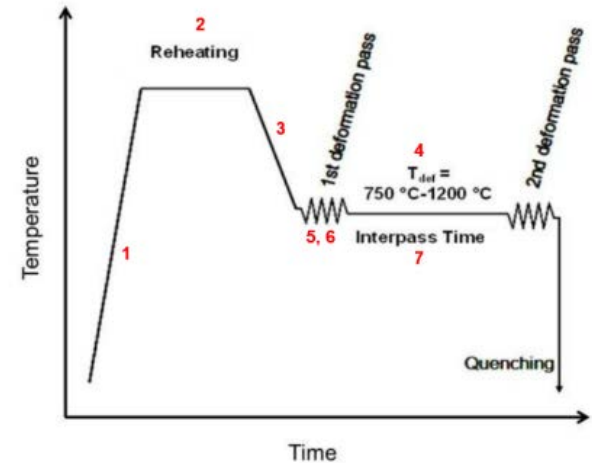
▲ Calculation of phase fraction using Thermo-Calc.

Alloy design – Thermo-mechanical processing

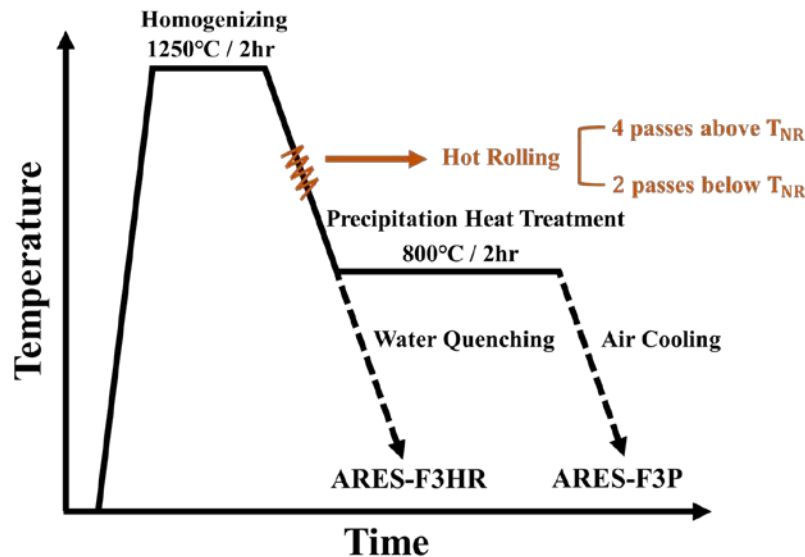
[1] C. N. Homsher, Colorado School of Mines (2012)

Thermo-mechanical processing (TMP) for TaC precipitation

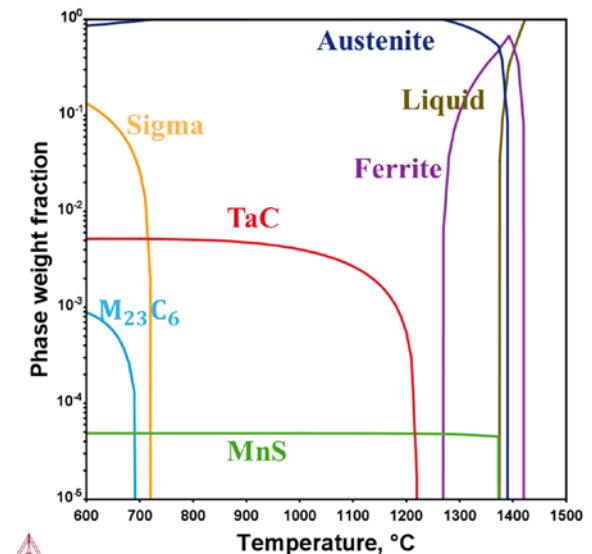
- Formation of **pre-existing dislocations** by hot-rolling
 - Utilizing the non-recrystallization temperature (T_{NR})
 - Double-hit deformation test
 - Nucleation site for TaC precipitates
- Precipitation** heat treatment
 - Ferrite forming temperature ($\sim 1270^\circ\text{C}$)
 - TaC forming temperature ($\sim 1220^\circ\text{C}$)



▲ Schematic of double-hit deformation test [1]



▲ Schematic of TMP for TaC precipitation

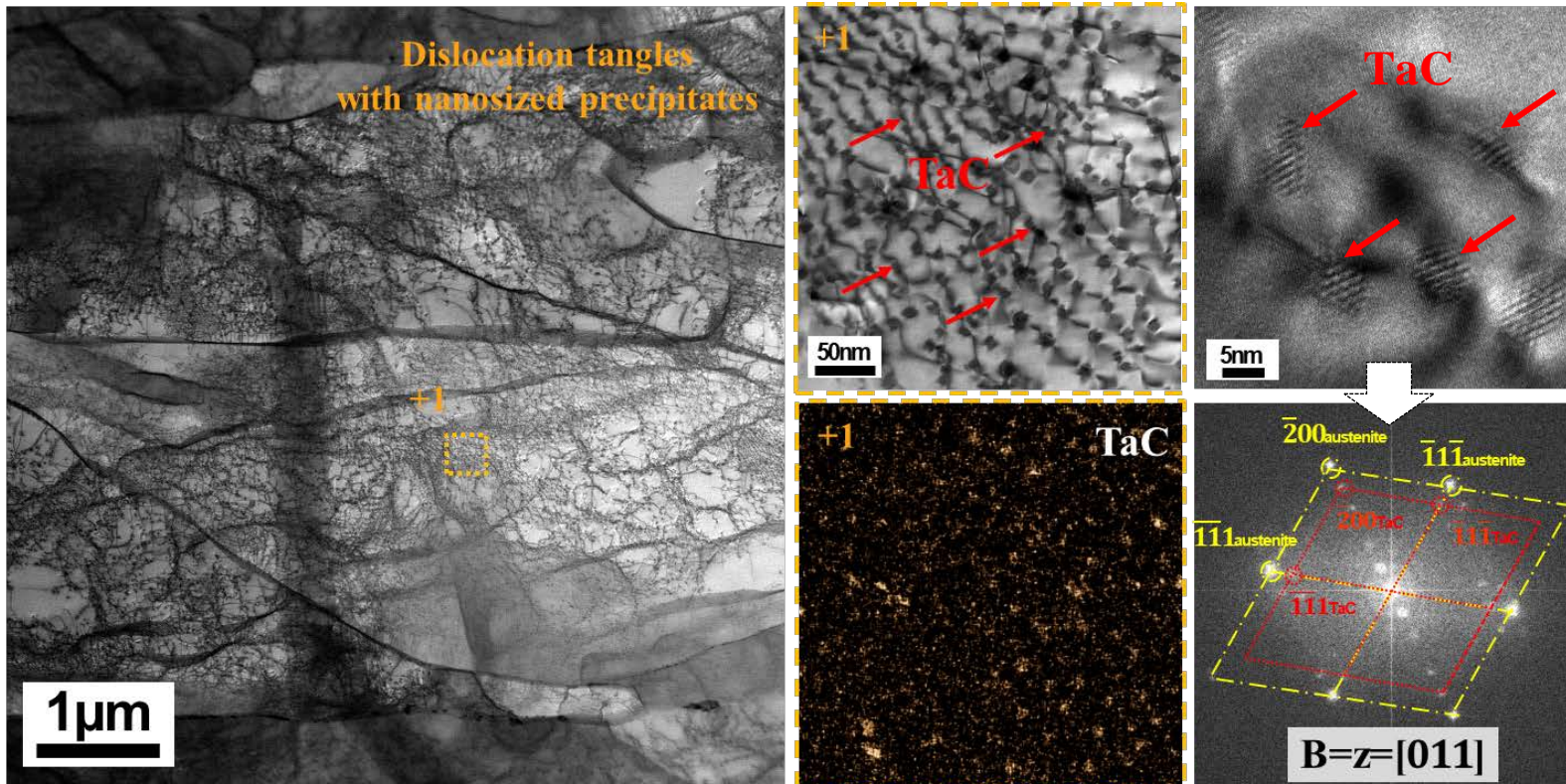


▲ Calculation of phase fraction using Thermo-Calc.

Alloy design – Thermo-mechanical processing

□ Microstructure of **ARES-F3P**

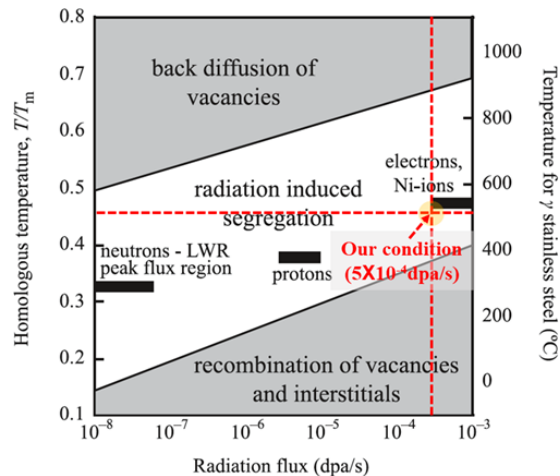
- High number density of TaC precipitates near pre-existing dislocation
- $\bar{\rho}_{\text{ppt}} = \sim 1.7 \times 10^{23} \text{ m}^{-3}$
- $\bar{D} = \sim 5.7 \text{ nm}$



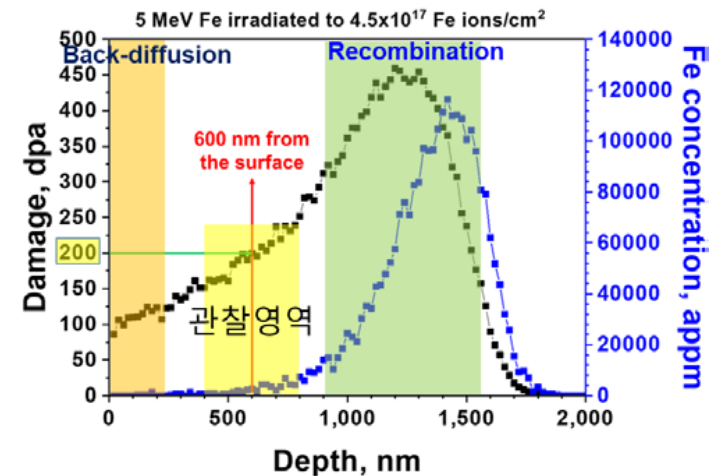
▲ TEM and EDS mapping images of ARES-F3P

□ Heavy ion irradiation for simulation of neutron irradiation

- Materials
 - ARES-F3P
 - Commercial 316 SS (Reference alloy)
- Irradiation condition
 - Stopping and Range of Ions in Matter (SRIM) simulation
 - 40eV displacement energy in Kinchin-Pease model (K-P model)
 - Targeted damage : **200 dpa** / Dose rate : 5×10^{-4} **dpa/s** at 600nm
 - **500°C** static defocusing beam with **Fe²⁺ ion**



▲ Heavy ion irradiation conditions [1]

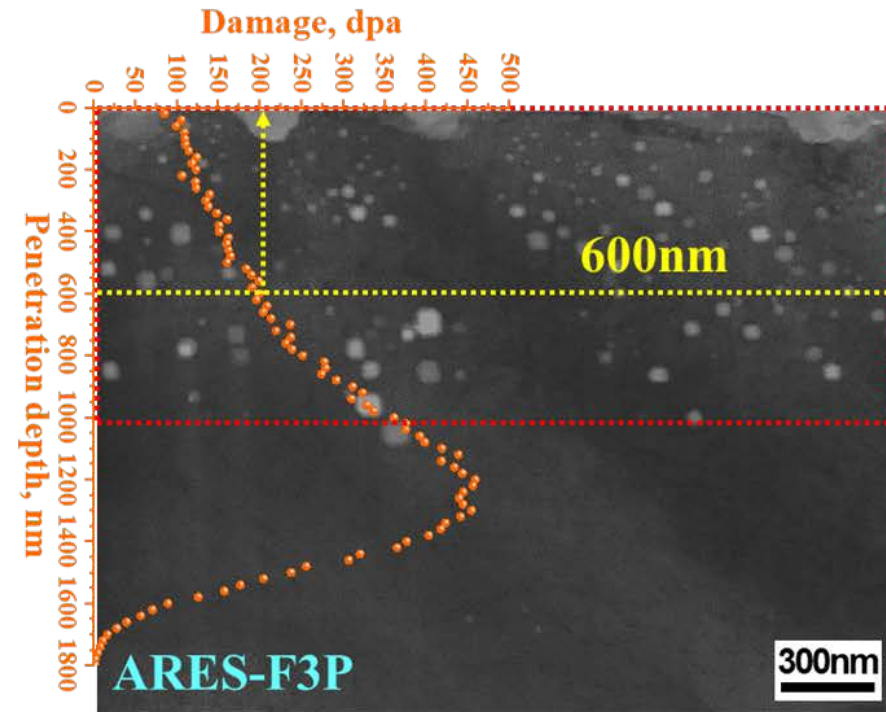
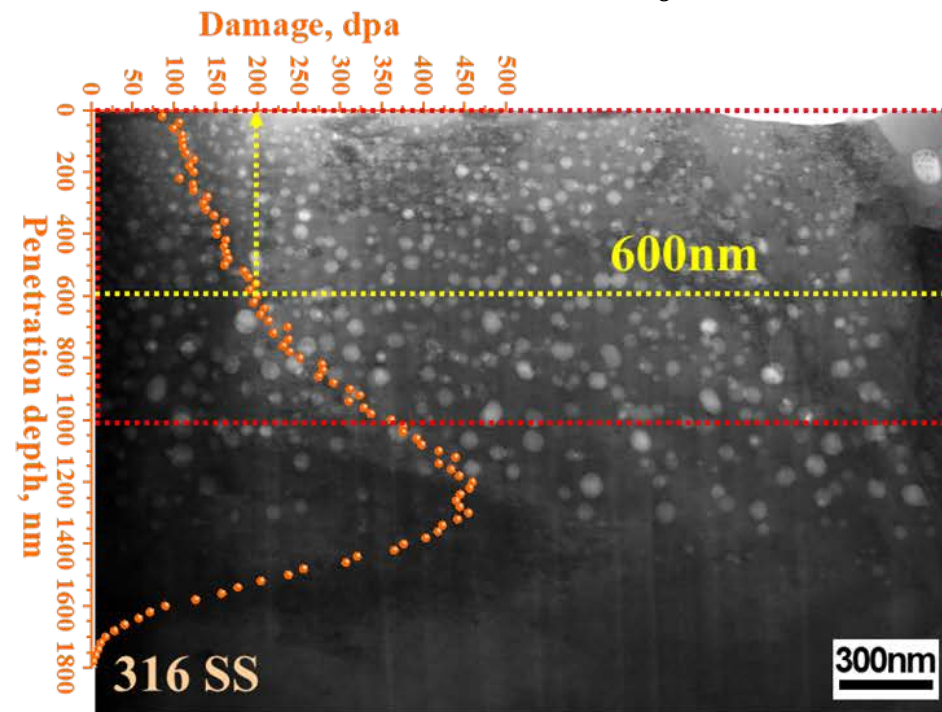


▲ Depth profile of radiation damage (dpa) based on SRIM simulation under K-P model

□ Void swelling measurement

- High-magnitude BFTEM images → Mainly 400 ~ 800 nm from the surface
- Void size & Void density measurement by Image-J software

- Void swelling (%) = $\frac{\frac{\pi}{6} \sum_{i=1}^N d_i^3}{A \times t - \frac{\pi}{6} \sum_{i=1}^N d_i^3} \times 100 - [1]$

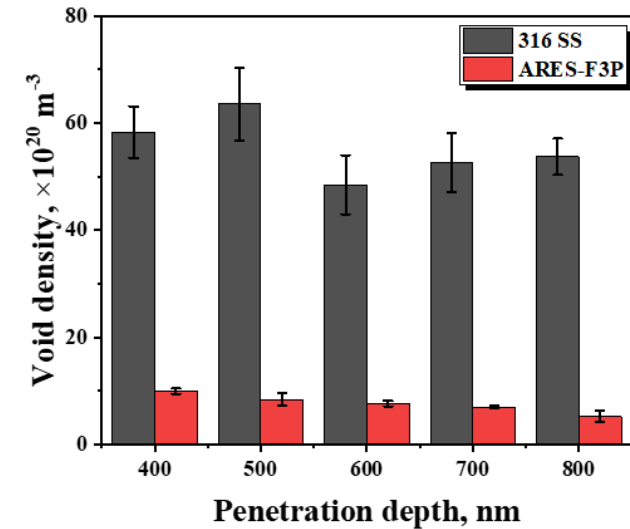


▲ Cross-sectional BFTEM images showing the voids in irradiated 316 SS and ARES-F3P

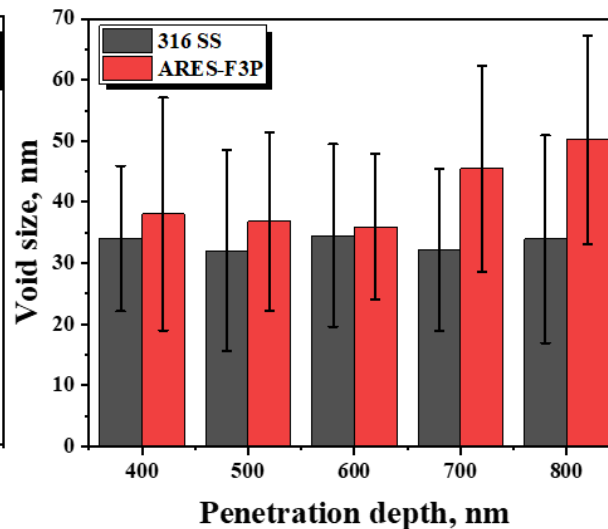
Void swelling resistance

□ Void swelling measurement

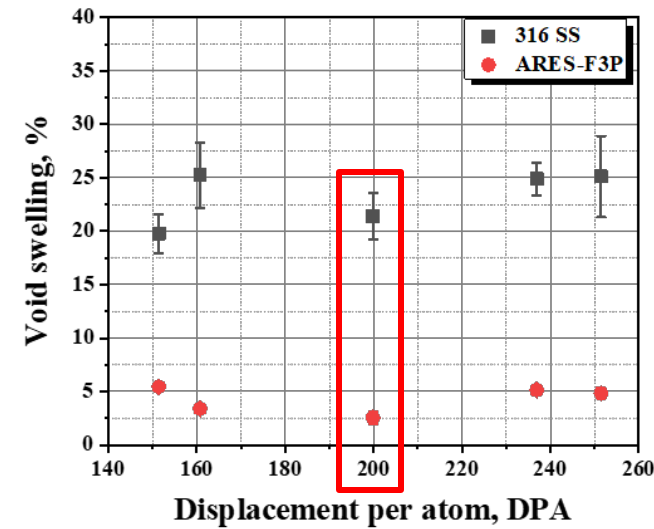
- High number density of voids for 316 SS
- Similar Void size
- **Much larger void swelling for 316 SS than ARES-F3P at 400 ~ 800 nm from the surface**



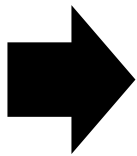
▲ Average void density of 316 SS and ARES-F3P



▲ Average void size of 316 SS and ARES-F3P



▲ Average void swelling of 316 SS and ARES-F3P



Uniformly distributed fine TaC precipitates in austenitic matrix
shows superior void swelling resistance

❑ Development of **ARES-F3**

- Fe-Ni-Mn-Cr system for **low activation** material
- **High radiation resistance** compared to commercial austenitic SS
 - Fully austenitic matrix
 - Uniformly distributed fine precipitates
- **Formation of TaC precipitates** near pre-existing dislocations through TMP
 - Hot-rolling based on double-hit deformation test
 - Precipitation heat treatment
 - $\bar{\rho}_{ppt} = \sim 1.7 \times 10^{23} m^{-3}$, $\bar{D} = \sim 5.7 nm$

❑ Void swelling resistance

- Heavy ion irradiation (~200 dpa: high damage level)
 - Radiation damage and dose rate selection based on SRIM under K-P model
 - **Void size and number density measurement** → **Void swelling**
 - Comparing ARES-F3P with reference 316 SS → **Superior void swelling resistance in ARES-F3P**



Energy for Earth !!



Thank you!

Appendix: Irradiation hardening

□ Irradiation hardening resistance by nano-indentation

- Materials

- ARES-F3P
- Commercial 316 SS (Reference alloy)

- Nano-indentation

- Small-scale evaluation method due to **shallow penetration depth** of ion irradiation
- Orowan dispersed barrier hardening (DBH) model
- **Much larger irradiation hardening for 316 SS than ARES-F3P**

$$\Delta H_v = 0.0945 \Delta H_0 \text{ (GPa)}$$

$$\Delta \sigma_y = 3.03 \Delta H_v \text{ (MPa)}$$

$$\Delta \sigma_{y,i} = M \alpha_i \mu b \sqrt{N_i d_i} \text{ (MPa)}$$

$$\Delta H_v = \frac{M \mu b}{3.03} \left(\sum \alpha_i^2 N_i d_i \right)^{1/2} \text{ (MPa)}$$

